Top Catal (2009) 52:1105–1115
DOI 10.1007/s11244-009-9250-0

ORIGINAL PAPER

Electronic Structure of Unsaturated V_2O_5(001) and (100) Surfaces: Ab Initio Density Functional Theory Studies

P. Hejduk · M. Witko · K. Hermann

Published online: 21 May 2009

Abstract Vanadium oxides based materials are well known to play an active role as catalysts in many chemical processes of technological importance like for example hydrocarbon oxidation reactions or selective catalytic reduction of NO_x in the presence of ammonia. Usually the (010) surface is pointed out as the most important, however one has to underline that other low-indices surfaces are by far less studied. In the present study the electronic structure of V_2O_5(001) and (100) surfaces are determined by ab initio DFT methods using gradient-corrected RPBE exchange-correlation functional. As models of surface sections different embedded $V_{14}O_{45}H_{20}$, $V_{14}O_{44}H_{18}$, and $V_{21}O_{65}H_{25}$ clusters are considered for the (001) surface and $V_{12}O_{40}H_{20}$, $V_{14}O_{46}H_{22}$, $V_{16}O_{52}H_{24}$ for the (100) surface. Detailed analyses of the electronic structure of each cluster are performed using charge density distributions, Mayer bond orders, electrostatic potential maps, character of frontier orbitals, and density of states (total as well as partial, atom projected). Results of the calculations show that overall negative charge of the surface oxygen sites scales with their coordination independent of the surface orientation. Terminal oxygen O(1) is charged the least negatively while doubly coordinated atoms –O(2) and O^e(2) have charge twice as large. This indicates that bridging (for (001) and (100) netplanes) and edging (only for (001) netplane) oxygen sites are more nucleophilic than terminal vanadyl sites, which becomes important in view of the reactivity of the different sites for surface chemical reactions. Vanadium atoms present at these surfaces are positively charged (electrophilic) and may play a role of electron acceptors. The unsaturated surfaces show a strong tendency to surface relaxation that manifest by large relaxation energies.

Keywords V_2O_5 · Electronic structure · Unsaturated surfaces · DFT

P. Hejduk · M. Witko (✉)
Institute of Catalysis and Surface Chemistry, Polish Academy of Sciences, Niezapominajek 8, 30-239 Cracow, Poland
e-mail: ncwitko@cyf-kr.edu.pl

P. Hejduk · K. Hermann
Fritz-Haber-Institut der Max-Planck-Gesellschaft, Faradayweg 4-6, 14195 Berlin, Germany

1 Introduction

Vanadium oxide based catalysts are of a great importance in many technological processes like the oxidation of SO_2 to SO_3, naphthalene or *o*-xylene to phthalic anhydride or *n*-butane to maleic anhydride, or the ammoxidation of propane to acrylonitrile [1–5]. The enormous chemical interest in vanadia and vanadia-based systems comes from their use as catalyst components, in particular in selective hydrocarbon oxidation reactions where oxygen from different surface sites participates in the reaction. Vanadia-based catalysts can be also applied in the protection of the natural environment i.e., in the selective catalytic reduction (SCR) of NO_x in the presence of ammonia [1, 6, 7]. Catalytic properties of vanadia may be connected with the fact that this material can expose different types of surfaces, those build of saturated vanadium (like the single crystal (010) surface) and those coordinatively unsaturated where surface ions accumulate excess charge and generate significant variations in the surface potential [8] (e.g., at (100) and (001) surfaces). The existence of these different V_2O_5 surface terminations together with different crystal

morphology might be a reason for vanadia catalysts supporting different catalytic reactions and yielding different products [9, 10].

As a first example of structure sensitive reaction the studies on methanol oxidation may serve [9], where by the slow recrystallisation and fusion monocrystalline grains of V_2O_5, exposing the (010), (100), and (001) faces with different percentage of each are obtained. Oxidation of methanol on these samples show that depending on the face orientation three products are observed. The V_2O_5 crystallite with dominantly (010) face yields the methylal whereas crystallites with lower (010) content lead to formaldehyde and ether. Another example is the isopropanol decomposition [10]. Here, the reaction can proceed via two routes: dehydrogenation to acetone or dehydration to propene. According to the experimental studies the (010) surface rich with terminal oxygen (basic sites) is mainly responsible for the acetone production whereas the activity of the faces with unsaturated vanadium ((001) and (100)) showing Lewis activity lead to the propene. Finally, studies on the selective catalytic reduction of NO_x in the presence of ammonia [11] using V_2O_5 crystallites with different morphology (different contents of low-index faces) show that V_2O_5 crystal grains with dominant (010) faces yield ammonia whereas grains exposing unsaturated faces are mainly responsible for the ammonia activation and NO_x reduction.

Obviously, the different reactivity of V_2O_5 low-index surfaces requires investigations of their electronic structure and sorption properties. So far, the theoretical work [7, 12–40] has focused mainly on the electronic structure, stability and reducibility, as well as adsorption ability of different molecules at the fully saturated (010) surface applying both cluster and periodic approaches at different levels of theory.

The large interest in the (010) surface properties can be explained by the layered structure of V_2O_5 bulk where atomic layers along the (010) direction are weakly bound and generate cleavage planes seen by AFM (Atomic Force Microscopy), as well as STM (Scanning Tunneling Microscopy) experiments [41, 42]. Also MD (Molecular Dynamic) simulations (based on electrostatic interactions) of the thermal stability of the V_2O_5 structure have indicated the (010) netplane as the most stable among the three low-index surfaces of V_2O_5 [43]. Theoretical investigations of the stability of (100) and (001) netplanes perpendicular to the (010) surface [44] have also shown that although their steadiness is an order of magnitude lower, their content in the structure of a standard crystal reaches 7.2 and 8.3%, respectively. For this reason, they should not be neglected. Moreover, the content of the above mentioned surfaces is expected to be larger in powder material.

In the present work the discussion concerning surface models and electronic structure of the (001) and (100) netplanes as well as the surface relaxation are considered. All results are compared with the data for the (010) surface obtained earlier but augmented by local relaxation of the clusters.

2 Computational Details

The crystal lattice of vanadium pentoxide is of an orthorhombic symmetry with a space group D_{2h}-P_{mmn} and unit cell parameters given by $a = 11.51$ Å, $b = 4.37$ Å, $c = 3.56$ Å [45–47]. The building unit forms a distorted octahedron with V–O bond distances varying between very short (1.58 Å, vanadyl groups) and very long (2.79 Å, Van der Waals type bonding). Three possible low-indices surfaces of V_2O_5 namely the (010), (001) and (100) are shown in Fig. 1.

The most stable (010) surface (Fig. 1a) is characterized by three structurally different oxygen sites: vanadyl oxygen atoms (O1), which stick out of the surface in rows and are singly coordinated to vanadium atom, and two bridging oxygen sites, doubly (O2) and triply (O3) coordinated to vanadium centers. The unsaturated (001) surface (Fig. 1b), which is described by mixture of "valley"- and "hill"-like regions exhibits coordinatively unsaturated vanadium (V^t) and three structurally different oxygen sites that lie in the netplane (Fig. 1b): vanadyl oxygen O(1) and bridging oxygen atoms O(2) or $O^e(2)$ (the second connected to V from different atomic layer) coordinated to two vanadium atoms, where the name "edging" $O^e(2)$ comes from its position at the edge of the surface towards the "valley"-like region. At the flat, most stable termination of the (100) surface (Fig. 1c) [44] unsaturated V as well as singly and double coordinated O sites are present at the planar surface.

To model V_2O_5(001) surface sections local clusters $V_{14}O_{45}H_{20}$, $V_{14}O_{44}H_{18}$ were cut out from the surface for "valley"- and "hill"-like surface regions (Fig. 2a), respectively. In addition a larger $V_{21}O_{65}H_{25}$ cluster describing both regions simultaneously was considered. The first smaller cluster characterizes the local environment of O(1), O(2) and V centers, whereas the second mimics the surroundings of the $O^e(2)$ center. In addition cluster $V_{21}O_{65}H_{25}$ allows investigation cluster size convergence.

For the V_2O_5(100) netplane the "t1" termination, which is characterized by unsaturated V atoms together with two kinds of oxygen sites (O(1) and O(2)), has been chosen as the most stable from among four possible cuts of this surface [44] and to simulate that surface systematic studies on $V_{12}O_{40}H_{20}$, $V_{14}O_{46}H_{22}$, $V_{16}O_{52}H_{24}$ clusters (Fig. 2b) were performed.

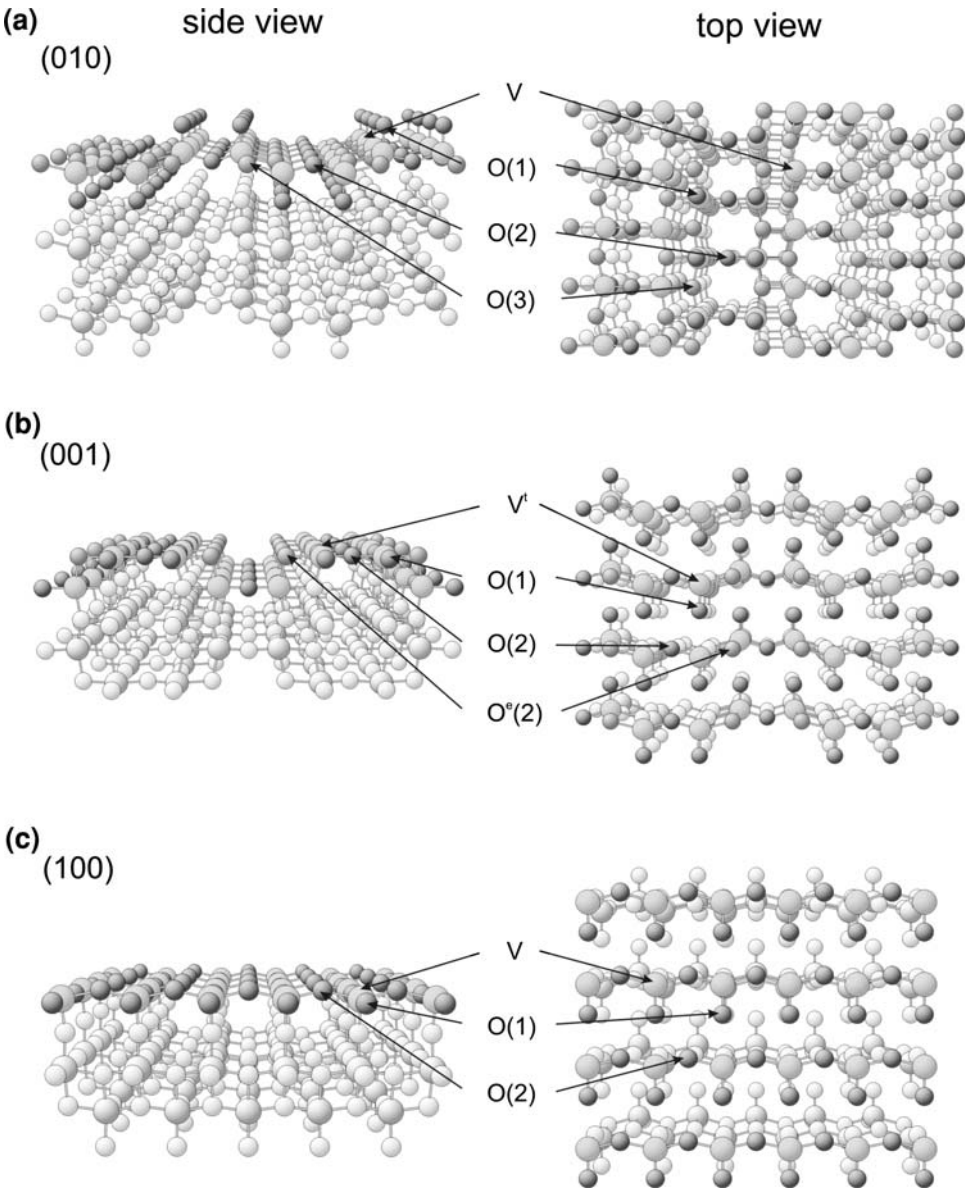

Fig. 1 Three low-index surfaces of vanadium pentoxide: **a** $V_2O_5(010)$, **b** $V_2O_5(001)$, and **c** the most stable "t1" termination for $V_2O_5(100)$ netplane [44]

In all clusters dangling bonds of peripheral oxygen were saturated by hydrogen forming OH groups and resulting in formally neutral clusters [19].

The electronic structure of the clusters was determined by ab initio density functional theory (DFT) methods where the Kohn-Sham orbitals were represented by linear combination of atomic orbitals (LCAO's) using all electron basis sets of contracted Gaussians obtained from atom optimizations [48, 49]. Electron exchange and correlation was described by a revised version of the gradient corrected functional due to Perdew-Burke-Ernzerhof (RPBE) [50, 51]. For the calculations the program StoBe was applied. Detailed analyses of the electronic structure of each cluster were performed using charge density distributions (Mulliken populations) [52], Mayer bond orders [53, 54], characteristic of frontier orbitals, total as well as partial atom projected densities of states and electrostatic potential maps.

Relaxation of the local environment near each oxygen site was allowed by corresponding geometry optimization. The local environment of a particular oxygen was defined by its nearest V neighbors together with oxygen linked with these atoms. The number and type of the atoms included in the relaxation are listed in the appropriate tables in the following paragraphs. The relaxation energy is then defined as:

$$E_{\text{relax}} = |E_{\text{tot}}(\text{relaxed cluster}) - E_{\text{tot}}(\text{isolated cluster})|, \quad (1)$$

where E_{tot}(isolated cluster) denotes the total energy of the cluster with atoms in bulk positions whereas E_{tot}(relaxed cluster) the total energy of the cluster after geometry

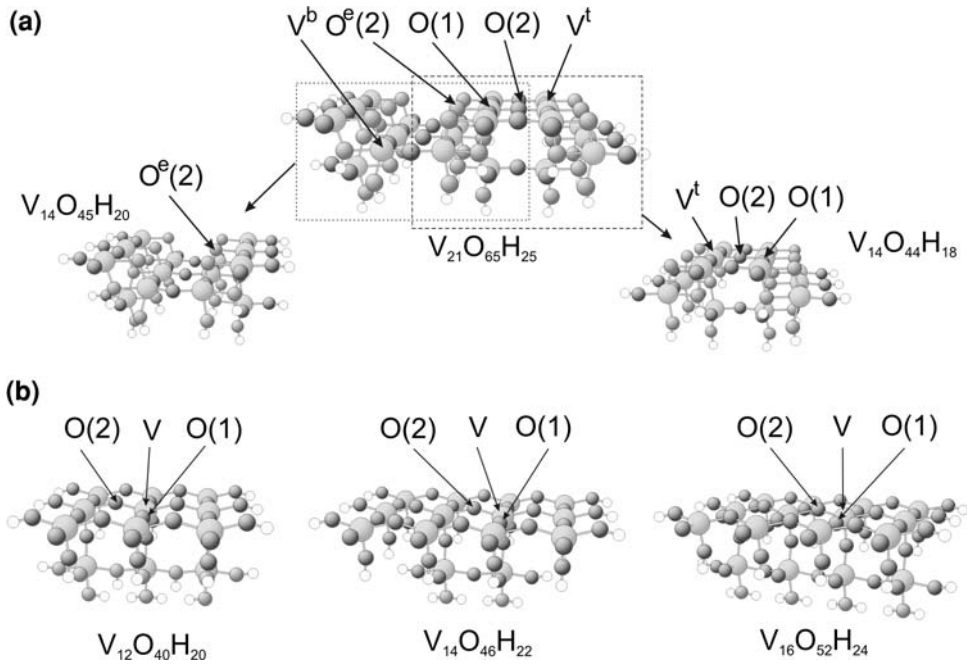

Fig. 2 Surface cluster models for unsaturated surfaces: **a** $V_2O_5(001)$ and **b** $V_2O_5(100)$ netplanes. All discussed oxygen and vanadium centers are labeled

optimization with equilibrium positions of the appropriate atoms.

3 Results and Discussion

3.1 The $V_2O_5(010)$ Surface Clusters

As mentioned before, the (010) surface was the main object in the theoretical studies of the V_2O_5 electronic structure. Both the cluster and periodic approximations [12, 13, 15–25, 28, 31, 32, 44, 55–59] were used at various levels of theory, starting from the semi-empirical methods, to DFT approach. To complete the structural description and to compare the (010) with (001), and (100) surface orientations, here some results obtained for the (010) termination are summarized and augmented by HOMO/LUMO characterization.

The present calculations (see Table 1 and Ref. [24, 25, 57]) show that atomic charges localized on oxygen and vanadium atoms differ substantially from their formal charges. Charges localized on the surface oxygen atoms scale with the coordination of these oxygen centers amounting to: −0.34/−0.69/−0.87 for O(1)/O(2)/O(3) sites. Positive charge localized at vanadium sites equals to 1.59. The Mayer bond order analyses yield a V=O(1) bond of order 2.06, two V–O(2)–V bonds of order 0.83 each and three bonds linking O(3) to three V sites of 0.49, 0.54, and

Table 1 Cluster $V_{10}O_{31}H_{12}$ modeling $V_2O_5(010)$. Atomic charges (q), V–O bond orders (p) and V–O bond distances (d) before and after geometric relaxation. Atoms involved in optimization are listed

$V_2O_5(010)$	$V_{10}O_{31}H_{12}$	Center relaxed		
		O(1)	O(2)	O(3)
q (V)	1.59	1.53	1.53	1.56
q (O(1))	−0.34	−0.34	−0.33	−0.33
q (O(2))	−0.69	−0.67	−0.67	−0.68
q (O(2))	−0.87	−0.84	−0.85	−0.83
p (V=O(1))	2.06	2.08	2.09	2.08
p (V–O(2))	0.83	0.84	0.86	0.87
p (V–O(3))	0.49	0.55	0.53	0.53/0.52/0.47
d (V=O(1))	1.59	1.59	1.58	1.59
d (V–O(2))	1.78	1.82	1.81	1.81
d (V–O(3))	1.88	1.91	1.90	1.90/1.99/2.04
E_{relax} [eV]	–	0.31	0.17	0.67
Atoms relaxed		V*6, O(1), O(2), O(3)*3	V*2, O(1)*2, O(2), O(3)*6	V*3, O(1)*3, O(2)*3, O(3), O(3)*4

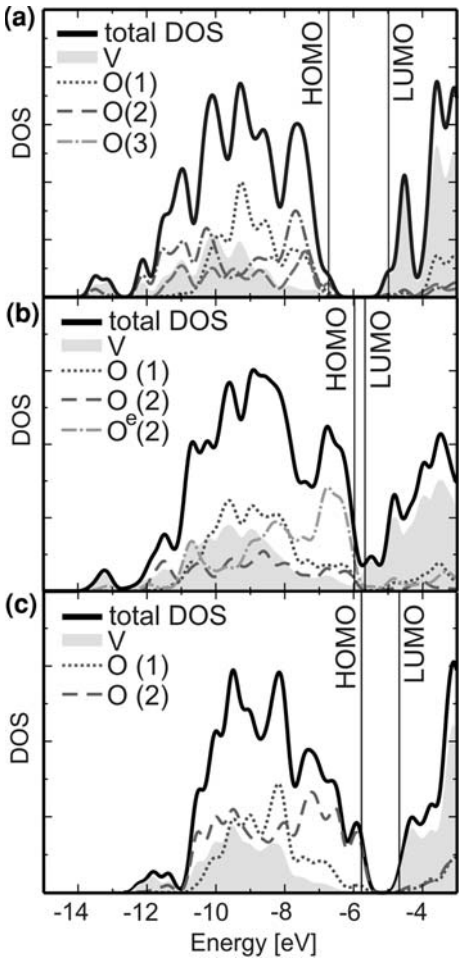

Fig. 3 DOS and pDOS plots for the valence region for the **a** $V_2O_5(010)$ surface obtained with the $V_{10}O_{31}H_{12}$ cluster, **b** $V_2O_5(001)$ surface obtained with the $V_{21}O_{65}H_{25}$ cluster and **c** $V_2O_5(100)$ surface obtained with the $V_{16}O_{52}H_{24}$ cluster

0.39 bond order. Together with the Mulliken analysis this indicates the mixed ionic-covalent nature of the V–O bonds. The most nucleophilic oxygen is located at the O(3) centre, followed up by O(2) and O(1), where the latter is the least nucleophilic.

The diagram of the density of states (see Fig. 3a and Ref. [24, 25, 57]) has a three-peak structure where peaks are identified as mixture of states localized both at metallic and oxygen centers. Electronic states of singly coordinated O(1) centers are found in the central part of the valence band and those from doubly- (O(2)) and triply(O(3)) coordinated oxygen cover the entire energetic region of the valence band with the highest concentration close to the Fermi level. The unoccupied electronic states are mainly localized at the metallic cations, which play the role of the acidic Lewis centers. The calculated width of the valence band is equal to about 0.6 eV [25] and this value is consistent with the experimental values, both from XPS and UPS experiments [23, 60]. The width of the energy gap for V_2O_5 bulk determined by photoemission experiments [61], optical adsorption [62] and optical reflectance [63] is equal to 2.35, 2.30, and 2.38 eV, respectively, which confirms its semiconductor nature. The theoretical gap values from DFT calculations for the crystal [22] and for the (010) surface amount to 1.9 eV and 2.1 eV and are surprisingly close to the experiments [61–63] in view of the deficiency of density functional theory to account for gap values in general.

The maps of electrostatic potential drawn for the 2 Å distance from the surface show only negative potential values, what indicates that only electrophilic or polarizable neutral particles may come close to the surface. The positive potential arising from metal centers is not visible therefore the approaching molecule "does not feel" the metallic centers.

The analysis of molecular orbital (Fig. 4) shows that the HOMO orbitals are localized mainly on the O(2) and O(3) centers indicating these centers as playing the main role of electron donors during the electrophilic attack. The LUMO orbitals are confined mostly on metallic centers suggesting them as electron acceptors in nucleophilic reaction.

Due to a weak interaction between layers and to a fact that all surface atoms are coordinatively saturated at the (010) surface and the surface is the most stable among the low-index V_2O_5 surfaces [43, 44], one should expect a practically zero effect of the surface relaxation. Table 1 lists changes in electronic parameters and bond distances due to relaxation of the different centers for the $V_{10}O_{31}H_{12}$ cluster. From the calculations one observes no significant changes in the electronic structures as a result of local surface relaxation. The relaxation causes also no differences in density of states and does not affect the nature of

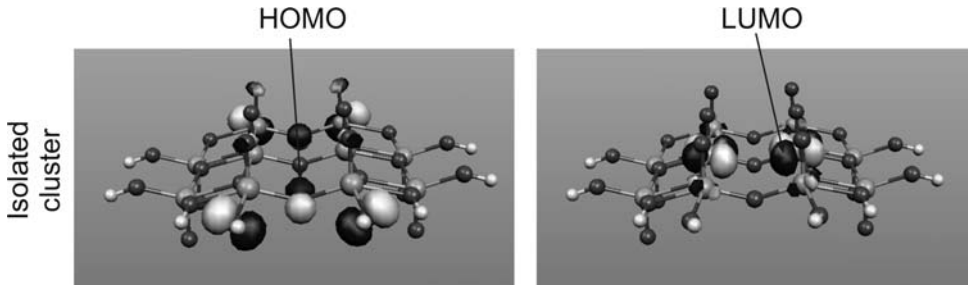

Fig. 4 The character of HOMO and LUMO orbitals for the $V_{10}O_{31}H_{12}$ cluster modeling the $V_2O_5(010)$ surface

frontier orbitals. The bond distances are slightly elongated due to relaxation; the largest change of the V–O distance reaches 0.11 Å and concerns the relaxation of three-fold oxygen O(3).

The local relaxation energy values, E_{relax}, equal to 0.31/0.17/0.67 eV for the O(1)/O(2)/O(3) centers, respectively, substantiate the little relaxation effect for the V_2O_5(010) surface.

3.2 The V_2O_5(001) Surface Clusters

As stated before, the electronic structure of the coordinatively unsaturated V_2O_5(001) surface has not been considered yet, either theoretically or experimentally. Therefore, the studies have started with the verification of appropriate cluster models. To model V_2O_5(001) surface the $V_{14}O_{45}H_{20}$, $V_{14}O_{44}H_{18}$ local clusters were used to represent "valley"- and "hill"-like surface regions (Fig. 2a), respectively. In addition, the big $V_{21}O_{65}H_{25}$ cluster, which describes both regions simultaneously, was taken into account to investigate the cluster size convergence.

Table 2 summarizes results of the Mulliken population and Mayer bond order analyses for the three above mentioned cluster models. Similarly as for the saturated (010) surface, atomic charges differ from their formal values, which indicates mixed ionic–covalent nature of surface bonds. The charge at the V^t- type vanadium atom (see Fig. 2a) is smaller than that of vanadium at the saturated surface and equals approximately to +1.3 (both for $V_{21}O_{65}H_{25}$ and $V_{14}O_{44}H_{18}$ clusters). Its smaller value may be explained by the fact that one of the neighboring oxygen atoms is missing, which causes that the electrons participating in the broken bond still reside on the cation. As a result, the V^t centers show the tendency to create new bonds, which may cost the enhanced adsorption on this surface. The charge of the V^b- type vanadium (both for $V_{21}O_{65}H_{25}$ and $V_{14}O_{44}H_{18}$ clusters, see Fig. 2a) is larger and equals to +1.6, which is consistent with the charges of metal centers on the (010) netplane and related to complete coordinative saturation of this center with O atoms.

The oxygen at the (001) surface are charged similarly as at the (010) surface; charges scale with the coordination number to V atom and amount to −0.37/−0.71/−0.61 for the O(1)/O(2)/O^e(2) centers. Thus, the most nucleophilic are oxygen atoms two-fold coordinated; their properties are similar to the same type of centers exposed at the (010) surface.

Table 2 contains also results of Mayer bond orders analyses indicating the type of V–O bonds, which depends on the coordination of the oxygen centers. The computed bond orders are approximately equal to 1.9, $2^*0.8$, 1 and 0.8, for V^t–O(1), V^t–O(2)–V^t, and V^t–O^e(2)–V^b bonds, which confirms mixed ionic–covalent nature of bonds on the V_2O_5(001) surface. The comparison of results obtained for the $V_{21}O_{65}H_{25}$ cluster (modeling a larger surface section) with the $V_{14}O_{44}H_{18}$ cluster (modeling the "mountain" region) and the $V_{14}O_{45}H_{20}$ cluster (modeling the "valley" region) proves the correctness of both smaller models. The charge on V^t and the bond orders for V^t=O(1) and V^t–O(2) are identical for the pair of the clusters: $V_{21}O_{65}H_{25}$ and $V_{14}O_{44}H_{18}$, while the charge on V^b and the bond orders for V^b–O^e(2) and V^t–O^e(2) remain the same in the $V_{21}O_{65}H_{25}$ and $V_{14}O_{45}H_{20}$ clusters.

The maps of electrostatic potential for the (001) surface (Fig. 5) show two distinct regions on the surface. The potential above the "hill"-like region, dominated by the coordinatively unsaturated vanadium atoms is positive

Table 2 Atomic charges (q) and bond orders V–O (p) for the central atoms for the $V_{21}O_{65}H_{25}$, $V_{14}O_{44}H_{18}$, and $V_{14}O_{45}H_{20}$ clusters of V_2O_5(001) surface

	$V_{21}O_{65}H_{25}$	$V_{14}O_{44}H_{18}$	$V_{14}O_{45}H_{20}$
q (V^t)	1.30	1.33	–
q (V^b)	1.61	–	1.60
q (O(1))	−0.37	−0.37	–
q (O(2))	−0.71	−0.71	–
q (O^e(2))	−0.60	–	−0.61
p (V^t–O(1))	1.91	1.91	–
p (V^t–O (2))	0.82	0.82	–
p (V^t–O^e(2))	0.99	–	0.99
p (V^b–O^e(2))	0.78	–	0.77

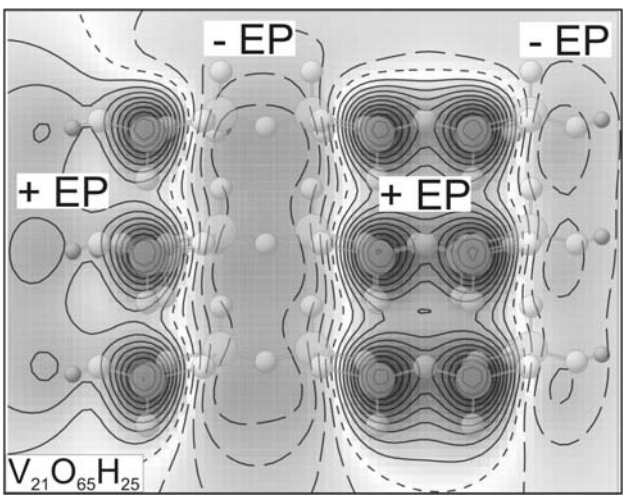

Fig. 5 The electrostatic potential map calculated at the distance of 2 Å above the V_2O_5(001) surface—projection from the above. Plot is obtained for $V_{21}O_{65}H_{25}$ cluster. The "+EP" and "−EP" denote positive and negative values of EP, respectively

indicating a possibility of the nucleophilic attack, i.e., the attack of a negatively charged molecule. The potential above the "valley"-like region, controlled by the $O^e(2)$ oxygen atoms is negative, allowing the electrophilic attack i.e., the attach of a positively charged molecule.

To complete the characterization of the electronic structure at the (001) surface, total and atom projected densities of states were evaluated for model clusters, where the results for the largest $V_{21}O_{65}H_{25}$ cluster is shown on Fig. 3b. Similar to the (010) surface all occupied states result from a mixing of 2sp-type orbitals of various surface oxygen atoms with smaller contributions from 3d-type orbitals of vanadium. The valence band is localized in the energy region between −12.73 and −5.98 eV. Its width is 6.75 eV, which corresponds to the width of the conductivity band obtained experimentally for the crystal [23, 60] and is close to value calculated for the (010) surface [25]. The states of the energy lower than −12.5 eV result from terminal OH groups in the cluster model and are therefore model artifacts. The main part of the spectrum has a multipeak structure, where the contribution of the single-coordinated O(1) oxygen atoms controls the central part of the band, of the double-coordinated O(2) oxygen atoms is uniformly distributed, whereas the input of the edge $O^e(2)$ oxygen atoms dominates close to the Fermi level. The unoccupied levels are characterized by 3d orbitals of vanadium. Such a spectrum clearly indicates the $O^e(2)$ atoms as the most reactive centers in the nucleophilic reaction (Lewis bases), while metal cations being the electron acceptors (Lewis acids).

The Lewis basic/acidic character of the $O^e(2)/V^t$ centers is also confirmed by the analysis of HOMO and LUMO orbitals (Fig. 6) where the HOMO orbital is localized mainly on $O^e(2)$ centers, whereas the contribution to the LUMO orbital comes almost exclusively from V^t centers.

The role of coordinatively unsaturated surface V atoms present at the (001) surface in surface relaxation was studied using the V_{14}- size clusters. Table 3 lists atomic charges as well as bond orders before and after the relaxation of the selected surface centers. However, there are no significant variations in electronic parameters due to surface relaxation, one notice changes in bond distances and much larger surface relaxation energy than in case of saturated (010) surface. Displacements of atoms from their bulk positions (changes in x, y, z atom coordinates) are pronounced and result in changes of bond distances (up to 0.2 Å). The greatest displacement (amounting to 0.62 and 0.55 Å) from atom bulk positions are observed for the double-coordinated O(2) and $O^e(2)$ centers whereas the average shift of O(1) atom is about 0.32 Å. Relaxation of one center (for example O(2)) causes not only changes in the bond involving this particular atom (elongation V^t–O(2) bond by 0.10 Å) but also influence other

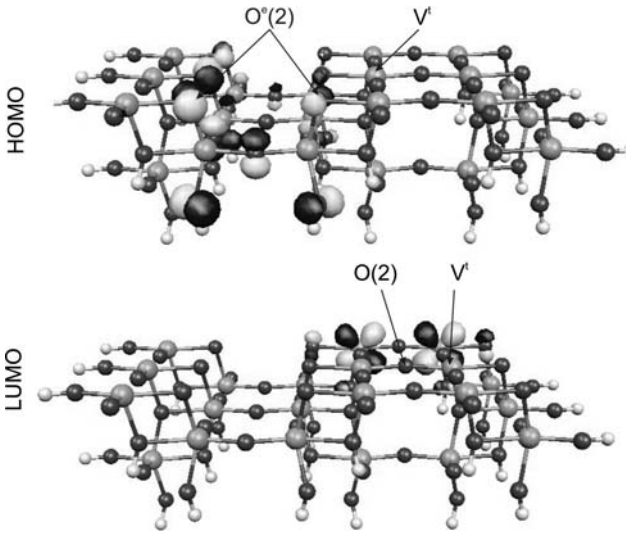

Fig. 6 The character of HOMO and LUMO orbitals for the different clusters modeling the $V_2O_5(001)$ surface obtained for the $V_{21}O_{65}H_{25}$ cluster

neighboring bonds; (shortening the V^t–O(2) by 0.22 Å and elongation of the V^b–$O^e(2)$ by 0.10 Å).

The values of local relaxation energies, E_{relax}, are equal to −1.53/−1.74/−0.91 eV for the O(1)/O(2)/$O^e(2)$ centers and can be related both to variations in the length of V–O bond lengths and also to the number of surface atoms that are optimized. Figure 7 presents the relaxation energy connected with optimization of different surface oxygen atoms as a function of the number of relaxed atoms, both from the surface and deeper layers. It is seen that the relaxation energy increases in a logarithmic way ($R^2 = 0.97$) with the number of relaxed surface atoms, and decreases following a power function ($R^2 = 0.96$) of the number of atoms from the deeper layers. Therefore, surface atoms are responsible for the (001) surface relaxation, whereas the atoms from deeper layers do not influence considerably the relaxation energy.

The considerable relaxation of the (001) surface, found using the cluster model has been confirmed with the periodic calculations [44], where the relaxation of the $V_2O_5(001)$ netplane of is accompanied by surface energy changing from 1.16 to 0.48 J/m^2 (decrease of 59%).

The electronic parameters describing the electronic structure of the $V_2O_5(001)$ surface, modeled by $V_{21}O_{65}H_{25}$ cluster and the corresponding two smaller $V_{14}O_{44}H_{18}V_{14}$ and $V_{14}O_{45}H_{20}$ clusters are in a very good agreement. In particular, charges of the respective centers, bond orders, electrostatic potentials determining the site and nature of the molecular attack at the surface and spectral characteristic of the density of states are similar. Therefore, one can conclude that both smaller clusters $V_{14}O_{44}H_{18}V_{14}$ and $V_{14}O_{45}H_{20}$ are sufficiently precise for the description of the

Table 3 Clusters $V_{14}O_{44}H_{18}$ and $V_{14}O_{45}H_{20}$ modeling $V_2O_5(001)$. Atomic charges (q), V–O bond orders (p) and V–O bond distances (d) before and after geometric relaxation. Atoms involved in optimization are listed (*PA* surface layer atoms, *BA* bulk atoms)

$V_2O_5(001)$	$V_{14}O_{44}H_{18}$	Center relaxed		$V_{14}O_{45}H_{20}$	Center relaxed
		O(1)	O(2)		$O^e(2)$
q (V^t)	1.33	1.36	1.36	1.23	1.21
q (O(1))	−0.37	−0.40	−0.41	−0.36	−0.42
q (O(2))	−0.71	−0.72	−0.72	−0.72	−0.73
q ($O^e(3)$)	−0.57	−0.60	−0.59	−0.61	−0.60
p (V^t =O(1))	1.91	1.90	1.88	1.95	1.91
p (V^t–O(2))	0.82	0.86	0.84	0.94	1.00
p (V^t–$O^e(2)$)	1.02	0.96	1.05	0.99	1.03
p (V^b–$O^e(2)$)	0.82	0.83	0.74	0.77	0.74
d (V^t=O(1))	1.59	1.61	1.61	1.59	1.61
d (V^t–O(2))	1.78	1.89	1.88	1.78	1.89
d (V^t–$O^e(2)$)	2.02	1.83	1.80	2.02	1.81
d (V^b–$O^e(2)$)	1.89	1.94	1.99	1.89	1.95
E_{relax} [eV]	–	1.53	1.74	–	0.91
Atoms relaxed		PA: V^t, V^t, O(1), O(2), $O^e(2)$	PA: V^t, V^t, O(1) × 2, O(2),$O^e(2)$ × 2		PA: V^t, O(1), O(2), O^e**(2)**
		BA: V^b, O(3)	BA: O(3) × 2		BA: V^b, O(3), $O^b(2)$, $O^b(1)$, $O^b(3)$

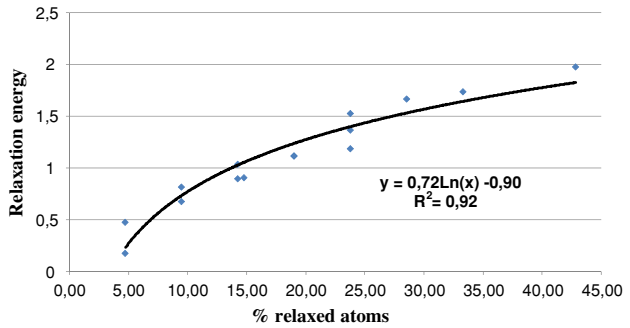

Fig. 7 The correlation plot of the relaxation energy as a function of the number of relaxed atoms

electronic structure of the (001) surface of V_2O_5, and in particular the activity of surface O(1), O(2), $O^e(2)$, and V^t centers.

3.3 The $V_2O_5(100)$ Surface Clusters

For the $V_2O_5(100)$ netplane the "t1" termination, characterized by unsaturated V atoms together with two kinds of oxygen sites (O(1) and O(2)), similarly as in the case of the (001) surface, different cluster models were examined to consider cluster size convergence and then to discuss electronic and geometric properties.

Table 4 collects the results of populations and bond orders (of the central cluster atoms, see Fig. 2b), where three clusters: $V_{12}O_{40}H_{20}$, $V_{14}O_{46}H_{22}$, and $V_{16}O_{52}H_{24}$ were selected as models of the (100) surface. Comparison of the results obtained for different clusters shows only weak dependence on cluster size and geometry; the largest deviation of electronic parameter being for the smallest cluster.

Results of population analyses performed for the $V_{16}O_{52}H_{24}$ cluster indicate that vanadium centers have Lewis acid character with charge equal to +1.39 that is closed to the V^t-type centers of the (001) netplane, which confirms the coordinative unsaturation of metallic centers at this netplane. Similarly to the (010) and (001) surfaces the nucleophilicity of surface oxygen sites increases with the coordination, qO(1) = −0.35, qO(2) = −0.71.

The bond order (1.95) for V=O(1) bonds indicate their double nature, while the V–O(2)–V bridges (bond orders of 0.83 and 0.83) are described by single bonds, with a greater ionic contribution that for V=O(1). Both, populations and bond orders do not yield noticeable differences between the (001) and (100) oriented surfaces.

Similar to the (001) surface, electrostatic potential maps for (100) netplane (Fig. 8) show surface regions of positive and negative potential, however these regions are not clearly separated. Thus, one can expect that the (100) surface will be attacked by the positive as well as negative particles, while neutral molecules may become polarized.

Table 4 Atomic charges (q) and bond orders V–O (p) for the central atoms for the clusters of V_2O_5(001) surface

	$V_{12}O_{40}H_{20}$	$V_{14}O_{46}H_{22}$	$V_{16}O_{52}H_{24}$
q (V)	1.42	1.38	1.39
q (O(1))	−0.36	−0.35	−0.35
q (O(2))	−0.72	−0.71	−0.71
p (V=O(1))	1.93	1.94	1.95
p (V–O(2))	0.82	0.83	0.83

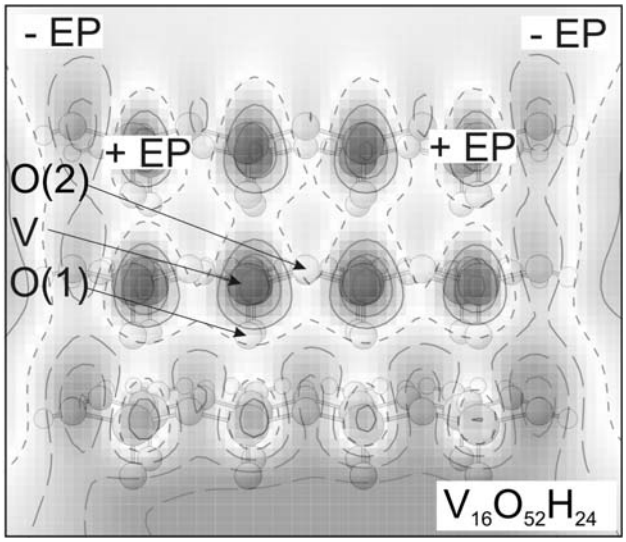

Fig. 8 The electrostatic potential map calculated at the distance of 2 Å above the V_2O_5(100) surface—projection from the above. Plot is obtained for $V_{16}O_{52}H_{24}$ cluster. The "+EP" and "−EP" denote positive and negative values of EP, respectively

Density of states for $V_{16}O_{52}H_{24}$ cluster plotted on Fig. 3c show no significant differences with respect to DOS calculated for the (010) and (001) surfaces that is to be expected taking into account that valence bands characterize bulk properties, hence being mostly independent of surface orientation.

From the nature of the HOMO and LUMO orbitals (determined for the V_{16} cluster) presented in Fig. 9 one observed that the HOMO orbitals are localized mainly on O(2) centers creating basic Lewis centers, while the LUMO orbitals are limited to V centers and play the role of electron acceptors.

The coordinatively unsaturated character of vanadium centers present at the (100) surface, similarly as in the case of the (001) surface, implicates the possibility of geometrical relaxation of this surface. The analysis of atomic charges and bond orders (see Table 5) shows that the local relaxation, similarly as for the (001) netplane, does not affect the electronic structure significantly. Both the largest change of atomic charges (0.06 for V) and of variation in the bond order (0.08 for V=O(1)) are insignificant. The density of states as well as character of frontier orbitals remain unchanged after the relaxation.

The relaxation causes shifts of atoms from their bulk positions (see Table 5) but displacements are small and lead to negligible changes in bond distances. The smaller relaxation energy obtained for cluster model of the (100) surface, in respect to the (001) surface, is confirmed by the periodic calculations [44] that show that the relaxation lowers the energy of the (100) surface from 0.61 to 0.55 J/m^2 only (decrease of 10%).

Although electronic characterization of the (100) surface obtained by its modeling via the V_{16} and V_{14} type clusters is very similar, the $V_{16}O_{52}H_{24}$ cluster should be consider for further studies on adsorption because that in the smaller cluster two V atoms from the second layer are missing, what may violate the electron density symmetry for the O(1) centre and may lead to erroneous description of the adsorption.

4 Summary: Saturated Versus Unsaturated V_2O_5 Surfaces

Results of the calculations carried out using the cluster approach prove that for each of the discussed low-index surfaces, systematic studies lead to the selection of the adequate cluster that can be used to model the surface. For the (010) surface it is the $V_{10}O_{31}H_{12}$ cluster, for the (001) surface—the $V_{21}O_{65}H_{25}$ (but also$V_{14}O_{44}H_{18}$ and $V_{14}O_{45}H_{20}$), and for the (100) surface—the $V_{16}O_{52}H_{24}$ cluster.

All studied surfaces have similar electronic structure and the surface V–O bonds are of a mixed, ionic-covalent nature. The nucleophilicity of O centers scale with their coordination number and depends upon their environment. On both unsaturated (001) and (100) surfaces charges on vanadium atoms are lower than on the saturated (010)

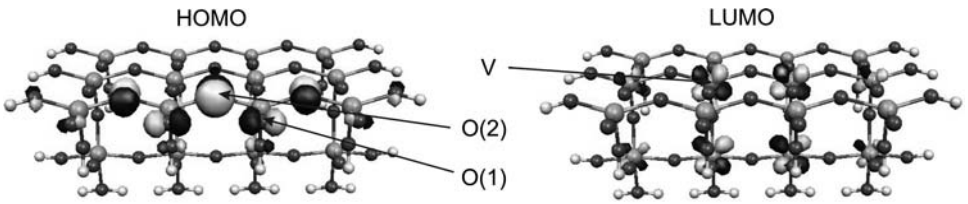

Fig. 9 The character of HOMO and LUMO orbitals for the $V_{16}O_{52}H_{24}$ cluster modeling the V_2O_5(100) surface

Table 5 Cluster $V_{16}O_{52}H_{24}$ modeling $V_2O_5(100)$. Atomic charges (q), V–O bond orders (p) and V–O bond distances (d) before and after geometric relaxation. Atoms involved in optimization are listed (*PA* surface layer atoms, *BA* bulk atoms)

$V_2O_5(100)$	$V_{16}O_{52}H_{24}$	Center relaxed	
		O(1)	O(2)
q (V)	1.39	1.37	1.33
q (O(1))	−0.35	−0.35	−0.33
q (O(2))	−0.71	−0.69	−0.68
p (V=O(1))	1.95	1.96	2.03
p (V–O(2))	0.83	0.86	0.86
d (V=O(1))	1.59	1.59	1.59
d (V–O(2))	1.88	1.92	1.91
E_{relax} [eV]	–	0.22	0.35
Atoms relaxed		PA: V, V, V, O(1), O(2), O(2)	PA: V, V, O(1), O(1), O(2), O(2), O(2)
		BA: O(2)	BA: O(2), O(2)

surface, which may enhance the activity of creating new ionic-covalent bonds at unsaturated surfaces.

Density of states spectra show large similarities in their multi-peak structure; the single-coordinated O(1) centers admixed with vanadium component control the middle part of the valence band, the O(2)/O^e(2) bridging atoms mixed with V are uniformly distributed over the entire band, while the contribution of O(2) for the (010) and (100) surfaces and of O^e(2) for the (001) surface dominate close to the Fermi level. The conductivity band is formed mainly by vanadium orbitals.

In all surfaces, the electron-acceptor sites (the Lewis acidic centers) are vanadium centers, while the basic Lewis sites are O(2), O^e(2), and O(3) centers.

The largest differences in the properties of the studied surfaces concern electrostatic potential maps. In contrast to the (010) surface, where only the nucleophilic attack is possible, the coordinatively unsaturated surfaces may be attacked both by positively and negatively charged molecules, because of the presence of positively and negatively charged regions on the surface.

The coordinatively unsaturated (001) and (100) surfaces are characterized by larger geometrical relaxation (variations in atoms position and in bonds length) than the saturated (010) surface; the relaxation effect is the largest for the (001) surface. The relaxation does not influence the electronic structure significantly.

Acknowledgments Financial supports by Polish Ministry of Science and High Education Grant No N204 024 31/0475 and by the Deutsche Forschungsgemeinschaft via Sonderforschungsbereich 546 "Transition Metal Oxide Aggregates", are gratefully acknowledged.

References

1. Grzybowska-Świerkosz B, Trifiro F (1997) Appl Catal A 157:1
2. Grzybowska-Świerkosz B (1997) Appl Catal A 157:263
3. Grzybowska-Świerkosz B (1997) Appl Catal A 157:409
4. Grzybowska-Świerkosz B (2000) Top Catal 11/12:23
5. Surnev S, Ramsey MG, Netzer FP (2003) Prog Surf Sci 73:117
6. Busca G, Lietti L, Ramis G, Berti F (1998) Appl Catal B 18:1
7. Calatayund M, Mguig B, Minot C (2004) Surf Sci Rep 55:169
8. Haber J, Witko M, Tokarz R (1997) J Appl Catal A 157:3
9. Volta JC, Portefaix JL (1985) Appl Catal 18:1
10. Grzybowska-Świerkosz B (1987) Mater Chem Phys 17:121
11. Ozkan US, Cai Y, Kumthekar MW, Zhang L (1993) J Catal 142:182
12. Witko M, Tokarz R, Haber J (1991) J Mol Catal 66:205
13. Witko M, Hermann K (1993) J Mol Catal 81:279
14. Witko M, Hermann K (1994) In: Corberan VC, Bellon SV (eds) Studies in surface science and catalysis, vol 82. Elsevier, Amsterdam, p 75
15. Witko M, Hermann K, Tokarz R (1994) J Electron Spectrosc Relat Phenom 69:89
16. Witko M (1996) Catal Today 32:89
17. Hermann K, Michalak A, Witko M (1996) Catal Today 32:321
18. Witko M, Tokarz R, Haber J (1997) J Appl Catal A 157:23
19. Michalak A, Witko M, Hermann K (1997) Surf Sci 375:385
20. Witko M, Tokarz R, Hermann K (1998) Polish J Chem 72:1565
21. Witko M, Hermann K, Tokarz R (1999) Catal Today 50:553
22. Chakrabarti A, Hermann K, Druzinic R, Witko M, Wagner F, Petersen M (1999) Phys Rev B 59:10583
23. Hermann K, Witko M, Druzinic R, Chakrabarti A, Tepper B, Elsner M, Gorschluter A, Kuhlenbeck H, Freund HJ (1999) J Electron Spectrosc Relat Phenom 98/99:245
24. Hermann K, Witko M, Druzinic R, Tokarz R (2000) Top Catal 11/12:67
25. Hermann K, Witko M, Druzinic R, Tokarz R (2001) Appl Phys A 72:429
26. Homann T, Bedrow T, Jug K (2002) Surf Sci 515:205
27. Sayede AD, Mathieu C, Khelifa B, Aourag H (2003) Mat Chem Phys 81:183
28. Yin X, Fahmi A, Endou A, Miura R, Gunji I, Yamauchi R, Kubo M, Chatterjee A, Miyamoto A (1998) Appl Surf Sci 130–132:539
29. Yin X, Han H, Endou A, Kubo M, Teraishi K, Chatterjee A, Miyamoto A (1999) J Phys Chem B 103:1263
30. Yin X, Han H, Gunji I, Endou A, Ammal SSC, Kubo M, Miyamoto A (1999) J Phys Chem B 103:4701
31. Brazdova V, Ganduglia-Pirovano MV, Sauer J (2004) Phys Rev B 69:165420
32. Ganduglia-Pirovano MV, Sauer J (2004) Phys Rev B 70:045422
33. Ganduglia-Pirovano MV, Hofmann A, Sauer J (2007) Surf Sci Rep 62:219

34. Sambeth J, Juan A, Gambaro L, Thomas H (1997) J Mol Cat A: Chem 118:283
35. Miyamoto A, Inomata M, Hattori A, Ui T, Murakami Y (1982) J Mol Catal 16:315
36. Gilardoni F, Weber J, Baiker A (1997) Int J Quantum Chem 61:683
37. Yin X, Han H, Miyamoto A (2000) Phys Chem Chem Phys 2:4243
38. Anstrom M, Dumesic JA, Topsøe N-Y (2002) Catal Lett 78:281
39. Soyer S, Uzun A, Senkan S, Onal I (2006) Catal Today 118:268
40. Hermann K, Witko M (2001) The chemical physics of solid surfaces. In: Woodruff DP (ed) Oxide surfaces, vol 9. Elsevier, Amsterdam, p 136
41. Da Costa A, Mathieu C, Barbaux Y, Poelman H, Dalmai-Vennik G, Fiermans L (1997) Surf Sci 370:339
42. Smith RL, Rohrer GS, Lee KS, Seo D-K, Whangbo M-H (1996) Surf Sci 367:87
43. Yin X, Endou A, Miura R, Fahmi A, Gunji I, Yamauchi R, Kubo M, Teraishi K, Miyamoto A (1999) Comp Mater Sci 14:114
44. Goclon J, Grybos R, Witko M, Hafner J, (2009) J Phys: Condens Matter 21:095008
45. Byström A, Wilhelmi KA, Brotzen O (1950) Acta Chem Scand 4:1119
46. Bachman HG, Ahmed FR, Barnes WH (1981) Z Kristallogr Kristallgeom Kristallphys Kristallchem 115:110
47. Wyckoff RWG (1965) Crystal structures. Interscience, Wiley, New York
48. Labanowski JK, Anzelm JW (eds) (1991) Density functional methods in chemistry. Springer, New York
49. Godbout N, Salahub DR, Anzelm J, Wimmer E (1992) Can J Phys 70:560
50. Perdew JP, Burke K, Ernzerhof M (1996) Phys Rev Lett 77:3865
51. Hammer B, Hansen LB, Nørskov JK (1999) Phys Rev B 59:7413
52. Mulliken RS (1955) J Chem Phys 23:1833, 1841, 2338, 2343
53. Mayer I (1983) Chem Phys Lett 97:270
54. Mayer I (1987) J Mol Struct (Theochem) 149:81
55. Witko M, Tokarz R, Haber J (1991) J Mol Catal 66:357
56. Haber J, Witko M (2003) J Catal 216:416
57. Witko M, Tokarz-Sobieraj R, Gryboś R (2005) Theoretical basis of the activation of light alkanes. Sustainable strategies for the upgrading of natural gas: fundamentals, challenges and opportunities. In: Derouane EG, Parmon V, Lemos F, Ramoa Ribeiro F (eds) NATO ASI Series II: Mathematics, Physics and Chemistry, vol 191. Springer, The Netherlands, p 85
58. Sayede D, Mathieu C, Khelifa B, Aourag H (2003) Mater Chem Phys 81:183
59. Sayede AD, Khelifa B, Pernisek M, Mathieu C, Aourag H (2004) Solid State Ionics 166:175
60. Shin S, Suga S, Taniguchi M, Fujisawa M, Kanzaki H, Fujimori A, Daimon H, Ueda Y, Kosuge K, Kachi S (1990) Phys Rev B 41:4993
61. Van Hieu N, Lichtman D (1980) J Vac Sci Technol 18:49
62. Cogan SF, Nguyen NM, Perrotti SJ, Rauh RD (1989) J Appl Phys 66:1333
63. Moshfegh AZ, Ignatiev A (1991) Thin Solid Films 198:251